Coupled-field description of zero-average dispersion management

C. Paré,[1,*] V. Roy,[2,†] F. Lesage,[3,‡] P. Mathieu,[2,†] and P.-A. Bélanger[1]
[1]*Centre d'Optique, Photonique et Laser (COPL), Département de Physique, Université Laval, Québec (Québec), Canada G1K 7P4*
[2]*Département de Physique, Université Laval, Québec (Québec), Canada G1K 7P4*
[3]*Centre de Recherches Mathématiques (CRM), Université de Montréal, Case Postale 6128, succursale A, Montréal (Québec), Canada H3C 3J7*
(Received 22 December 1998)

Using a coupled-field formalism and a standard perturbation analysis, we analyze a dispersion-managed system under zero-average dispersion conditions. A nonlinear integral equation in the spectral domain allows the determination of the critical strength parameter of a two-step dispersion map. Higher-order correction terms confirm the difference observed in the pulse shapes in each fiber and comparisons with fully numerical results reveal a good agreement. The existence of an antisymmetric dispersion-managed soliton is also confirmed. [S1063-651X(99)05109-0]

PACS number(s): 42.81.Dp, 42.65.Tg

I. INTRODUCTION

The possibility of upgrading, at a reduced cost, already installed standard fiber communication systems by having recourse to the technique of dispersion management has rapidly attracted a great deal of attention [1,2]. Reduction of the Gordon-Haus jitter [1–3] and the four-wave mixing crosstalk between the different channels of a wavelength-division-multiplexed system [4] are among the noteworthy features of this approach. However, the optimization of future dispersion-managed links still requires further numerical and analytical modeling, as the so-called ''dispersion-managed (DM) soliton'' reveals unusual properties when compared with the conventional nonlinear Schrödinger (NLS) soliton. In particular, as discussed by various groups [5–12], a DM soliton can sustain stable propagation in a zero- or normal-average dispersion link, as long as the ''map strength'' parameter is above some critical value S_{cr} [13]. A wavelength-division-multiplexed communication system is likely to operate in both anomalous and normal dispersion regimes and the zero-average dispersion case can, therefore, be viewed as an important frontier deserving further investigation. This is the subject of this paper.

In the *linear limit*, under total dispersion compensation, the evolution of the intensity profile of the pulse is identical in both fiber segments of a two-step dispersion map. This suggests that a perturbative approach, based on the definition of two dependent variables, one of them involving the small difference between the envelopes of the pulses in each fiber, might prove fruitful. To exploit this observation, we then introduce in this paper a *bilocal* change of variables which is reminiscent of a similar approach used thoroughly in the context of the quantum Hall-effect subject to a point contact and in the Kondo model as well [14,15], where it is referred to as *folding*. Although this change of variables may look simple, its nonlocality leads however to a nontrivial coupled-field description of dispersion management. Our analysis shows that, at the leading order, the spectrum of the DM soliton obeys a nonlinear integral equation whose solution can serve, for one, to extract the value of the critical parameter S_{cr}. The next order of perturbation implies a difference in the pulse profiles at the midpoint of each fiber segment and this is well confirmed by the numerical simulations. More generally, the comparison with fully numerical results reveals an excellent agreement. The analysis also confirms the prediction based on another approach [16] concerning the existence of an *antisymmetric* DM soliton.

The paper is organized as follows. In Sec. II, a coupled-field description of dispersion management is introduced. In the absence of exact analytical solutions, a perturbative analysis is then carried out in Sec. III, leading to a nonlinear integral equation for the spectral distribution. The results are discussed and compared with numerical simulations in Sec. IV. The solution of the integral equation is shown to allow the determination of the critical parameter S_{cr} and the existence of an antisymmetric DM soliton is pointed out. A general discussion concludes the paper.

II. COUPLED-FIELD DESCRIPTION

We consider a two-step dispersion map (Fig. 1) which consists of the periodic alternance of two fiber segments of length L_j $(j=1,2)$ and dispersion parameters $\beta_{2j}(\beta_{21}<0,\beta_{22}>0)$. Considering a zero-average dispersion $(\beta_{21}L_1=-\beta_{22}L_2)$, the propagation in the anomalous (first) and normal (second) fiber segments is described by the nonlinear Schrödinger (NLS) equation:

$$i\frac{\partial U_1}{\partial z_1}+\frac{1}{2}\frac{\partial^2 U_1}{\partial \tau^2}+|U_1|^2U_1=0, \tag{1a}$$

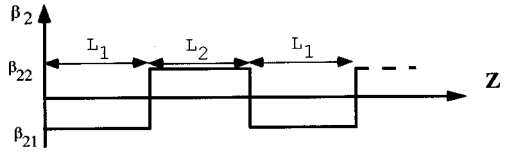

FIG. 1. Schematic representation of a two-step dispersion map.

*Author to whom correspondence should be addressed. FAX: (418) 656-2623. Electronic address: cpare@phy.ulaval.ca
†FAX: (418) 656-2040.
‡FAX: (514) 343-2254.

$$i\frac{\partial U_2}{\partial z_2}-\frac{1}{2}\frac{\partial^2 U_2}{\partial \tau^2}+r|U_2|^2U_2=0. \tag{1b}$$

The scaled variables $z_j=Z_j/L_{Dj}$ represent the propagation distances in terms of the local dispersion lengths $L_{Dj}=T_0^2/|\beta_{2j}|$, T_0 being a characteristic time scale; $0<z_j<l$, where $l=L_1/L_{D_1}=L_2/L_{D_2}$. The time τ is in units of T_0 and the fields are expressed in terms of the peak amplitude of the conventional NLS soliton that would propagate in the anomalous fiber. The ratio $r=(\gamma_2 L_2)/(\gamma_1 L_1)$ has been introduced, where $\gamma_{1,2}$ is the nonlinear parameter of the fibers. We restrict the present analysis to the lossless case.

In the stationary regime here considered, except for a residual uniform nonlinear phase shift θ, the pulse profile is perfectly reproduced after each period of the map. Furthermore, the phase profile of the field is uniform at the midpoint of each fiber; without loss of generality, we then impose a real field at $z_1=l/2$ (this is further validated below). The governing Eqs. (1a), (1b) then imply that the fields satisfy the following continuity and periodicity conditions:

$$U_1(z_1=0,\tau)\equiv U_0(\tau), \tag{2a}$$

$$U_1(z_1=l,\tau)=U_0^*(\tau), \tag{2b}$$

$$U_2(z_2=0,\tau)=U_1(z_1=l,\tau)=U_0^*(\tau), \tag{2c}$$

$$U_2(z_2=l,\tau)=\exp(i\theta)U_1(z_1=0,\tau)=\exp(i\theta)U_0(\tau). \tag{2d}$$

The phase shift θ can be viewed as a signature of the nonlinearity. Noting that in the *linear limit* ($\theta=0$) the fields in each fiber are simply related by $U_2^*(z_2=z,\tau)=U_1(z_1=z,\tau)$, we then introduce, with a perturbative treatment in mind, the following change of variables:

$$\psi_\pm(z,\tau)\equiv\frac{U_1(z,\tau)\pm U_2^*(z,\tau)}{2}. \tag{3}$$

We note an alternative interpretation of this transformation; since, in the same linear limit, $U_2(l-z,\tau)=U_2^*(z,\tau)$, this change of variables is strictly equivalent to a folding of the first half of the map onto the second half and this evokes a similar technique used for analyzing quantum impurity problems [14,15]. In these problems, the folding is allowed to uncover the integrability of the governing systems and this was not so clear in the original formulation. Here, the coupled system does not seem to be integrable although some conserved quantities can be found [17].

The new set of variables makes it possible to analyze the problem in terms of two fields coupled over the common domain $0<z<l$:

$$\begin{aligned}i\frac{\partial\psi_\pm}{\partial z}+\frac{1}{2}\frac{\partial^2\psi_\pm}{\partial\tau^2}=&-\frac{1}{2}[(1-r)(|\psi_\pm|^2\psi_\pm+2|\psi_\mp|^2\psi_\pm\\&+\psi_\mp^2\psi_\pm^*)+(1+r)(|\psi_\mp|^2\psi_\mp\\&+2|\psi_\pm|^2\psi_\mp+\psi_\pm^2\psi_\mp^*)]\end{aligned} \tag{4}$$

with the associated boundary conditions

$$\psi_+(z=0)=U_0, \tag{5a}$$

$$\psi_+(z=l)=\frac{[1+\exp(-i\theta)]}{2}U_0^*, \tag{5b}$$

$$\psi_-(z=0)=0, \tag{5c}$$

$$\psi_-(z=l)=\frac{[1-\exp(-i\theta)]}{2}U_0^*. \tag{5d}$$

The symmetric case ($r=1$) has received particular attention in the numerical work published so far. For this reason, and also because of the resulting reduction in the complexity of Eq. (4), we first investigate that case. We briefly discuss of the case $r\neq 1$ in the conclusion.

III. PERTURBATIVE ANALYSIS

To our knowledge, there is no exact analytical solution of the system (4), (5) that is of any relevance for the present analysis. However, in the regime of strong dispersion management, the dispersion dominates (*locally*) over the nonlinearity. This implies that, typically, the amplitude is small, $|U_0|\ll 1$, and this then suggests a perturbative analysis in terms of a small parameter, e.g., $\varepsilon\approx|U_{0\,\max}|^2$. For this purpose, we define $\psi_\pm=\sqrt{\varepsilon}V_\pm$ and $U_0=\sqrt{\varepsilon}V_0$, with $V_\pm$ and V_0 of order unity; we will return to the original variables later on. Equation (4) (with $r=1$) is then appropriately rewritten as

$$i\frac{\partial V_\pm}{\partial z}+\frac{1}{2}\frac{\partial^2 V_\pm}{\partial\tau^2}+\varepsilon(|V_\mp|^2V_\mp+2|V_\pm|^2V_\mp+V_\pm^2V_\mp^*)=0. \tag{6}$$

We can now proceed with a standard perturbative analysis and expand the fields $V_\pm$ and the phase shift θ as

$$V_\pm(z,\tau)=V_\pm^{(0)}(z,\tau)+\varepsilon V_\pm^{(1)}(z,\tau)+\varepsilon^2V_\pm^2(z,\tau)+\cdots, \tag{7a}$$

$$\theta=0+\varepsilon\theta_1+\varepsilon^2\theta_2+\cdots. \tag{7b}$$

(The zero-order phase shift has been set to zero so as to fall back on the correct linear limit.) The boundary condition (5a), combined with Eq. (7a), then implies

$$V_0=V_+(z=0)\equiv V_{00}+\varepsilon V_{01}+\varepsilon^2V_{02}+\cdots. \tag{7c}$$

This simply expresses the fact that the pulse profile at the fiber junction, in the stationary state, is also power dependent. We limit the present investigation to the terms in ε^1. At the leading order, the system is governed by the following linear homogeneous equations:

$$i\frac{\partial V_\pm^{(0)}}{\partial z}+\frac{1}{2}\frac{\partial^2 V_\pm^{(0)}}{\partial\tau^2}=0, \tag{8}$$

subject to the boundary conditions [read off Eq. (5)]:

$$V_+^{(0)}(0)=V_{00};\quad V_+^{(0)}(l)=V_{00}^*,$$

$$V_-^{(0)}(0)=0;\quad V_-^{(0)}(l)=0. \tag{9}$$

It proves convenient to solve Eq. (8) in the spectral domain. For this purpose, we introduce the Fourier transform $\tilde{h}(\nu) = \int h(\tau)\exp(-i2\pi\nu\tau)d\tau$. Then,

$$\tilde{V}_-^{(0)}(z,\nu)=0,$$

$$\tilde{V}_+^{(0)}(z,\nu)=\exp[-i2\pi^2\nu^2(z-l/2)]\varphi(\nu), \tag{10}$$

where $\varphi(\nu)$ represents the spectrum of $V_+^{(0)}$ at the midpoint $z=l/2$. At this order, the propagation is linear and *any real* function $\varphi(\nu)$ will ensure that the boundary condition $V_+^{(0)}(l)=V_+^{(0)*}(0)$ is satisfied. The selection appears at the next order where the equations to be solved read as

$$i\frac{\partial V_+^{(1)}}{\partial z}+\frac{1}{2}\frac{\partial^2 V_+^{(1)}}{\partial\tau^2}=0, \tag{11a}$$

$$i\frac{\partial V_-^{(1)}}{\partial z}+\frac{1}{2}\frac{\partial^2 V_-^{(1)}}{\partial\tau^2}=-|V_+^{(0)}|^2V_+^{(0)} \tag{11b}$$

with the boundary conditions [read off Eq. (5)]:

$$V_+^{(1)}(0)=V_{01};\quad V_+^{(1)}(l)=V_{01}^*-i\frac{\theta_1}{2}V_{00}^*,$$

$$V_-^{(1)}(0)=0;\quad V_-^{(1)}(l)=i\frac{\theta_1}{2}V_{00}^*. \tag{12}$$

By inspection, one finds that the first-order correction to the field V_+ is given, in the spectral domain, by

$$\tilde{V}_+^{(1)}(z,\nu)=-i\frac{\theta_1}{4}\tilde{V}_+^{(0)}(z,\nu)$$

$$=-i\frac{\theta_1}{4}\exp[-i2\pi^2\nu^2(z-l/2)]\varphi(\nu). \tag{13}$$

So, $V_{01}=-i(\theta_1/4)V_{00}$. Still in the spectral domain, the inhomogeneous Eq. (11b) yields

$$\tilde{V}_-^{(1)}(z,\nu)=\frac{1}{4\pi^2}\times\exp[-i2\pi^2\nu^2(z-l/2)]\int\int d\nu_1 d\nu_2\times\frac{\exp[i4\pi^2\nu_1\nu_2 z]-1}{\nu_1\nu_2}\exp[-i2\pi^2\nu_1\nu_2 l]\times\varphi(\nu+\nu_1)\varphi(\nu+\nu_2)\varphi(\nu+\nu_1+\nu_2), \tag{14}$$

where we have used the fact that φ is a real function. A compatibility condition arises when one wants to satisfy the boundary condition for $V_-^{(1)}(l)$ [Eq. (12)]. This condition translates into the selection of a particular solution φ (or a limited set) expressed mathematically in terms of a nonlinear integral equation. Coming back to the original variables, the latter reads as

$$\int\int d\nu_1 d\nu_2\frac{\sin[2\pi^2 l\nu_1\nu_2]}{2\pi^2 l\nu_1\nu_2}\Phi(\nu+\nu_1)\Phi(\nu+\nu_2)\times\Phi(\nu+\nu_1+\nu_2)=\lambda\Phi(\nu), \tag{15a}$$

where $\Phi=\sqrt{\varepsilon}\varphi$ represents, at the leading order, the spectral profile of the fields $U_{1,2}$ at $z_{1,2}=l/2$. The eigenvalue λ is simply related to the nonlinear phase shift by

$$\lambda=\frac{\theta}{2l}. \tag{15b}$$

Hence θ, the nonlinear phase shift incurred over one period, appears as a natural choice of parameter for characterizing a particular stationary DM soliton.

Equation (15), combined with Eqs. (10), (13), and (14), allows the description of the fields in each fiber. We are particularly interested in the pulse profile at the midpoint of each fiber and at their junction as well. Keeping terms in ε^1, in the spectral domain these profiles are given by

(i) in the middle of the first (anomalous) fiber segment

$$\tilde{U}_1(z_1=l/2,\nu)\cong\Phi(\nu)+J(\nu), \tag{16}$$

where

$$J(\nu)\equiv\frac{1}{2}\int\int d\nu_1 d\nu_2\frac{1-\cos[2\pi^2 l\nu_1\nu_2]}{2\pi^2 l\nu_1\nu_2}\Phi(\nu+\nu_1)\times\Phi(\nu+\nu_2)\Phi(\nu+\nu_1+\nu_2); \tag{17}$$

(ii) in the middle of the second (normal) fiber segment

$$\tilde{U}_2(z_2=l/2,\nu)\cong(1+i\theta/2)\Phi(\nu)-J(\nu), \tag{18a}$$

$$\cong\exp(+i\theta/2)\Phi(\nu)-J(\nu); \tag{18b}$$

(iii) at the junction

$$\tilde{U}_{12}(\nu)\equiv\tilde{U}_1(z_1=0,\nu)=\tilde{U}_2^*(z_2=0,\nu)$$

$$\cong(1-i\theta/4)\exp(+i\pi^2 l\nu^2)\Phi(\nu), \tag{19a}$$

$$\cong\exp(-i\theta/4)\exp(+i\pi^2 l\nu^2)\Phi(\nu). \tag{19b}$$

On physical grounds, the change $(1+i\theta/2)\rightarrow\exp(i\theta/2)$ in Eq. (18b) [and similarly for Eq. (19b)] is expected to improve the accuracy of the approximate analysis as it correctly implies that the first-order correction due to the nonlinearity mostly consists in a phase shift and, from symmetry considerations, the latter should be half of the total shift incurred over one complete period. This is well confirmed by the numerical results reported below.

IV. DISCUSSION AND NUMERICAL EXAMPLES

Equations (15)–(19) call for a few comments. First, we note that the nonlinear integral equation (15) is equivalent to the recent result of Ablowitz and Biondini [18] who based their analysis on the method of multiple scales [19]. We believe that besides being rather straightforward for analyzing the stationary state, the present analysis also has the ben-

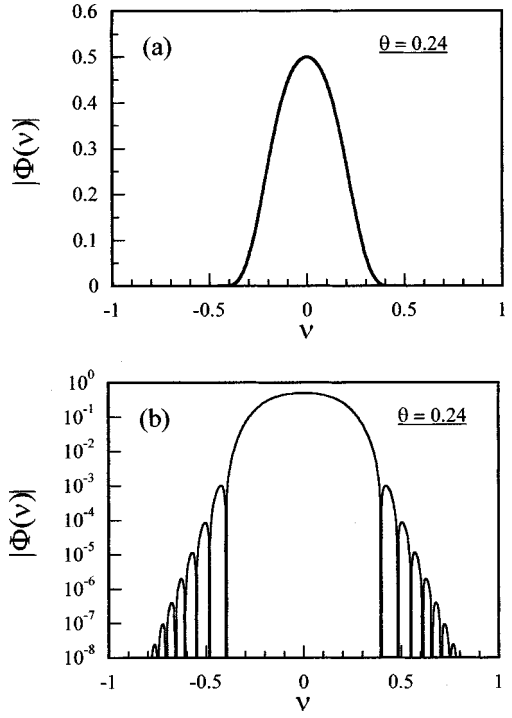

FIG. 2. (a) Spectral distribution $\Phi(\nu)$ corresponding to the eigenvalue $\lambda=0.019$ (see text). (b) Same as (a) but on a logarithmic scale. The parameters are $\beta_{22}=-\beta_{21}=10\ \mathrm{ps}^2/\mathrm{km}$; $L_1=L_2=80\ \mathrm{km}$ and the nonlinear phase shift is $\theta=0.24$. The frequency ν is in units of $1/T_0$.

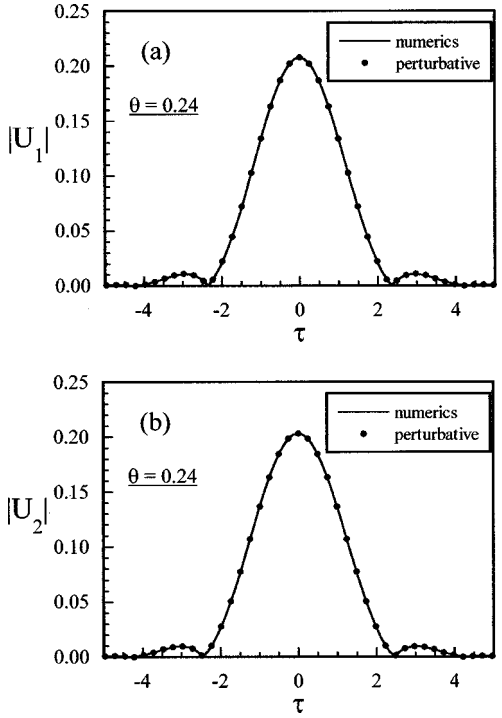

FIG. 3. Temporal distributions $|U_1|$ (a) and $|U_2|$ (b) at the midpoint of each fiber for the case $\theta=0.24$. The predictions of the perturbative analysis (dots) are compared with the exact numerical results based on Eq. (1) (solid lines). The time τ is in units of T_0.

efit of easily providing expressions for the next order of perturbation. This higher-order correction demonstrates, according to Eqs. (16) and (18), the nonlinearity-induced asymmetry observed in the evolution of the pulse in the two fibers.

Second, one can notice that Eq. (16) correctly predicts a real field at the midpoint of the anomalous fiber, as assumed in the derivation of Eq. (15). Equation (18), however, implies a small nonuniformity of the phase profile at the center of the second fiber. A proper inclusion of higher-order terms would remedy this.

Third, as pointed out by Ablowitz and Biondini [18], Eq. (15) obeys a scaling rule: if, for a given normalized length l_1,$\Phi_1(\nu)$ is a solution of Eq. (15) with an eigenvalue λ_1, then a new parameter $l_2=\alpha l_1$ will yield $\Phi_2(\nu)=\beta\Phi_1(\sqrt{\alpha}\nu)$ as a solution, with the eigenvalue $\lambda_2=(\beta^2/\alpha)\lambda_1$, β being an arbitrary factor. The phase shifts associated with these two solutions are then related by $\theta_2=\beta^2\theta_1$, the full width half maximum (FWHM) of the temporal intensity distribution at the midpoint of the anomalous fiber $\tau_{1/2}$ by $(\tau_{1/2})_2=\sqrt{\alpha}(\tau_{1/2})_1$ and the pulse energy E scales as $E_2=(\beta^2/\sqrt{\alpha})E_1$. In terms of the so-called ''*map strength*'' parameter S, here equal to $S=2|\beta_{21}|L_1/\tau_{1/2}^2=2l(T_0/\tau_{1/2})^2$ [this parameter was introduced by Smith *et al.* [1,8,10] and the reader is referred to that work for a discussion of its physical meaning; in the present symmetric case, one can notice that it is directly related to the ratio (fiber segment length)/(dispersion length) and thus gives an idea of the importance of the linearly induced pulse broadening in each fiber], this scaling law implies that, at this order, the solutions corresponding to different energies are characterized by the *same* strength parameter ($S_2=S_1$). Since this order of approximation corresponds to the quasilinear limit, this implies that in the diagram of the pulse energy E vs S, the corresponding points approach the S axis vertically at a value representing the critical parameter ($S_2=S_1\equiv S_{\mathrm{cr}}$). In the zero-energy limit (total absence of nonlinear effects), *any* pulse profile is perfectly reproduced after each period; in other words, any point on the S axis is then a solution. Introducing a small nonlinearity ($E\neq 0$) leads to the selection of a particular point on the S axis located at S_{cr} so that the latter, in this sense, can be viewed as a bifurcation point. The impact of the nonlinearity generally depends on the pulse shape and it is only for a particular pulse profile that the path-averaged interplay between dispersion and nonlinearity simply results in a uniform phase shift of the pulse spectrum after each period. (Further discussion on the physical interpretation of the critical parameter can be found in Ref. [10].) To determine the value of the critical parameter, we solved the integral equation (15) numerically, using an iterative scheme with a proper renormalization step to ensure a quick convergence to the solution (further details will be given elsewhere). The FWHM of the temporal intensity distribution, given by the square of the Fourier transform of $\Phi(\nu)$, implies a critical value $S_{\mathrm{cr}}\cong 3.76$. [This is in good agreement with the approximate value of 3.9 reported by Bernston *et al.* [8,13,20] and apparently extrapolated from purely numerical results—based on Eq. (1)—obtained for low, but finite, energy. We also note that the fact that the strength parameter involves the square of the inverse of the FWHM makes it strongly dependent on the pulse shape.] As pointed out in Sec. V, this value does not depend on the ratio r.

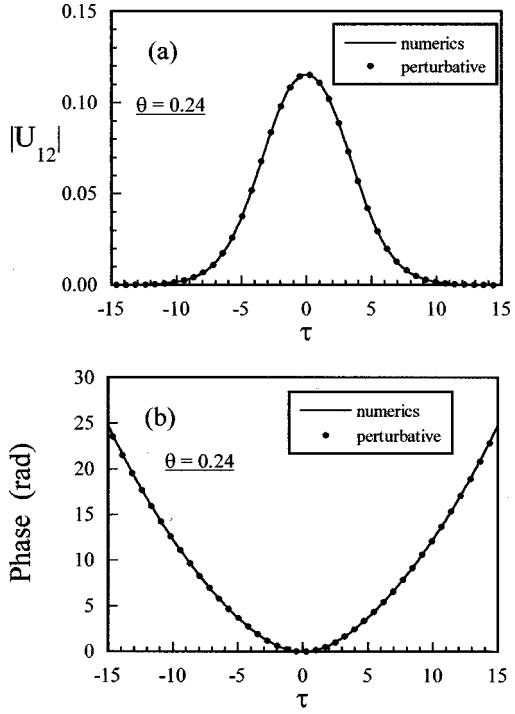

FIG. 4. Temporal distribution at the junction of the fibers for the case $\theta=0.24$ (a) amplitude profile $|U_{12}|$; (b) phase profile (a uniform phase has been removed at the pulse center). The predictions of the perturbative analysis (dots) are compared with the exact numerical results based on Eq. (1) (solid lines). Same normalization as Fig. 3.

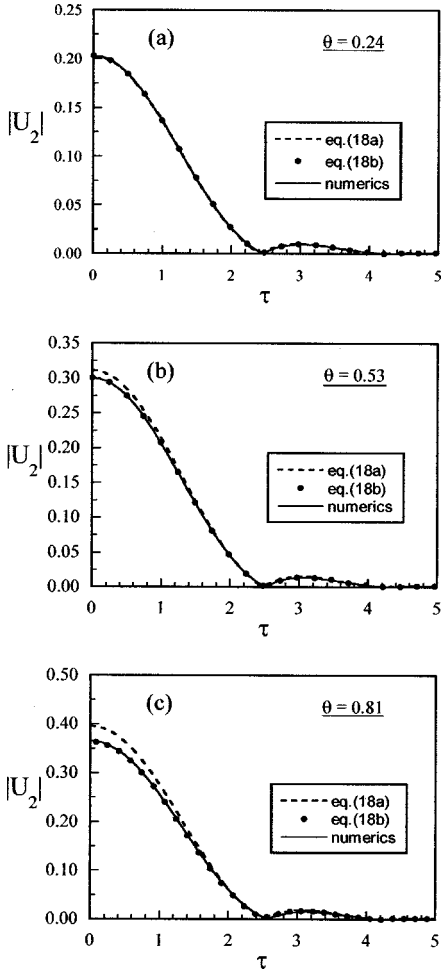

FIG. 5. Amplitude distribution $|U_2|$ at the midpoint of the *normal* fiber for various values of the nonlinear phase shift θ. The predictions of Eqs. (18a) (dashed lines) and (18b) (dots) are compared with the exact numerical results based on Eq. (1) (solid lines). Same normalization as Fig. 3.

Fourth, as shown below, Eq. (15) also admits an antisymmetric solution, implying that a DM system can sustain the propagation of a DM soliton of either even or odd parity. The existence of an antisymmetric stationary pulse shape has been predicted and numerically confirmed recently, using a different approach [16].

The rest of this section is concerned with the accuracy of the perturbative analysis when compared with the results of numerical simulations of a DM system based on Eq. (1). We consider, as an example, a communication link with the following parameters: $L_1=L_2=80\,\mathrm{km}$ with $\beta_{22}=-\beta_{21}=10\,\mathrm{ps}^2/\mathrm{km}$. The parameter $T_0=11.35\,\mathrm{ps}$, implying that a conventional NLS soliton $\mathrm{sech}\,\tau$ in the anomalous fiber would have a FWHM$=1.763\ T_0=20\,\mathrm{ps}$. The normalized length is then equal to $l=6.21$.

As a first example, we consider a case where the nonlinear phase shift $\theta=0.24$. Figure 2(a) first depicts the spectral distribution $\Phi(\nu)$ corresponding to the eigenvalue $\lambda=\theta/2l=0.019$ and obtained by solving Eq. (15) numerically. A logarithmic plot [Fig. 2(b)] reveals the presence of numerous tiny sidelobes. Sidelobes also prevail in the temporal domain when looking at the pulse profile at the midpoint of each fiber span, as shown in Fig. 3. The most notable feature of Fig. 3 is certainly the good accuracy of the perturbation analysis, as evidenced by the comparison between the exact numerical results based on Eq. (1) (solid lines) and the predictions of Eqs. (16) and (18) (dots). The peak amplitude of about 0.2 represents, in physical units, a peak power of 1.2 mW which is typical for a communication link. The prediction at the fiber junction [Eq. (19)] is also well confirmed by the numerics, as seen in Fig. 4. In particular, the quasiparabolic phase profile of field U_{12} is accurately reproduced by the perturbative analysis [Fig. 4(b)].

In Figs. 3(b) and 4(a) and 4(b), Eqs. (18b) and (19b) have been used, respectively. To better estimate the limits of the validity of the analysis, Fig. 5 now compares the predictions concerning the pulse shape $U_2(l/2,\tau)$ [Eqs. (18a) and (18b)] with the exact numerical results for various values of θ (similar conclusions prevail for the pulse shapes U_1 and U_{12}). Although Eqs. (18a) and (18b) are equivalent, to first order in θ, Eq. (18b) is clearly more accurate for describing the *amplitude* distribution $|U_2|$, even for relatively large phase shifts θ. Equation (18b) is still, however, limited in accuracy as it predicts a *nonuniform* phase profile, as shown in Fig. 6; more precisely, the perturbative result smooths out the π phase steps at the zeros of the amplitude distribution [see Fig. 5(c)]. Higher-order perturbation terms would correct this. We note, though, that the phase in Fig. 6 is quasiuniform in the central part of the pulse where most of the energy is concentrated.

As mentioned above, it turns out that the integral equation (15) also admits a solution of *odd* parity. For example, Fig. 7 displays the spectral distribution $\Phi(\nu)$ and the pulse profile $U_1(\tau)$ for the same system parameters as above and for a

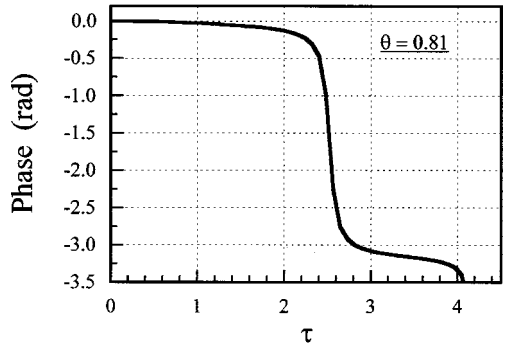

FIG. 6. Phase profile at the midpoint of the *normal* fiber span as predicted from Eq. (18b) for the case $\theta=0.81$. A constant phase shift has been removed at the pulse center. The exact phase profile is uniform except for a π phase step at the zeros of the amplitude distribution. Same normalization as Fig. 3.

nonlinear phase shift $\theta=0.24$. Whereas the pulse shape in Figs. 3 and 4 is, roughly speaking, Gaussian-like in its central part, the odd-parity solution depicted in Fig. 7 can be viewed as a distorted version of the next Hermite-Gauss function. Figure 8 demonstrates that this pulse shape is robust enough for propagating without further distortions over thousands of kilometers. Figure 8(b) represents another confirmation of the validity of the perturbative analysis. This result also supports the prediction of the existence of antisymmetric DM solitons based on an approximate ordinary differential equation for the DM soliton pulse shape [16]. Further simulations are being carried out in order to determine under which conditions the existence of this stationary

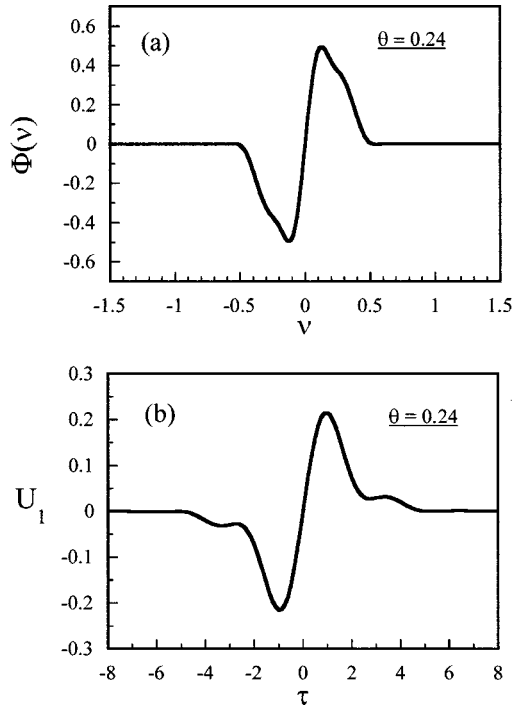

FIG. 7. Antisymmetric DM soliton as predicted from the perturbative analysis. (a) corresponding spectral distribution $\Phi(\nu)$; (b) temporal profile U_1 at the midpoint of the *anomalous* fiber span. The parameters are the same as in Fig. 2. The frequency ν is in units of $1/T_0$ and the time τ is scaled to T_0.

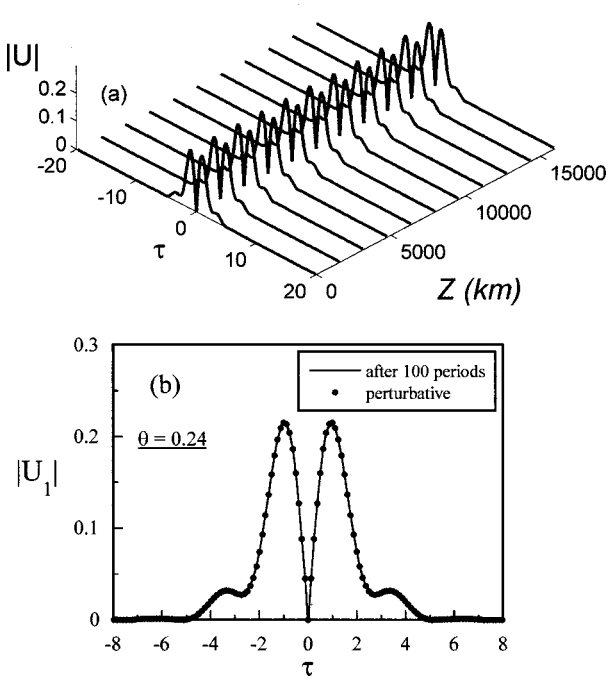

FIG. 8. (a) Stroboscopic view of the long-haul propagation (100 periods of the dispersion map) of the antisymmetric DM soliton along the communication link. The simulation is based on Eq. (1) and the pulse profile is shown at every ten periods; (b) comparison between the launched pulse (dots) corresponding to the perturbative prediction shown in Fig. 7(b) and the pulse profile after a propagation over 100 periods (solid line). The time τ is in units of T_0.

pulse shape could be the subject of an experimental confirmation. Let us mention for now that such simulations have already indicated that, just as with conventional soliton systems, one can cope with the losses of a real link by a proper boost of the input amplitude parameter in order to compensate for the reduction of the path-averaged peak power. This numerical analysis is in progress and the results will be detailed elsewhere.

V. CONCLUSION

Adopting a coupled-field approach and limiting ourselves to the stationary regime, we have analyzed dispersion management under zero-average dispersion conditions. Defining appropriate boundary conditions and using a standard perturbation analysis, a nonlinear integral equation has been derived for the spectral distribution of the pulse at the midpoint of each fiber, at the leading order. The analysis represents an interesting alternative to the multiple-scale method; it also easily includes higher-order correction terms that accurately reproduce the difference in the pulse shapes in each fiber.

We believe that the proposed analysis is particularly well suited for the determination of the critical parameter S_{cr} (corresponding to the zero-energy limit), since it is based on the asymptotic *linear* limit and treats the nonlinearity as a small perturbation. Most of the analysis here presented deals with the symmetric case $r=1$. However, the perturbative treatment leading to Eq. (15) can easily be repeated for the general case $r\neq 1$; one then finds that the integral equation (15) still prevails, except for the minor modification $\lambda\rightarrow[(1+r)/2]\lambda$. According to the scaling law mentioned above,

this implies that the critical parameter S_{cr} evaluated in the previous section does not depend on the map asymmetry, in agreement with the recent *numerical* results reported by Bernston *et al.* [20]. The analysis is, however, more involved at the next order of perturbation as Eq. (11a) then becomes *inhomogeneous*.

Except for very small sidelobes, the spectral distribution $\Phi(\nu)$ that satisfies the nonlinear integral equation and is depicted in Fig. 2 is approximatively Gaussian in shape. This suggests the possibility of deriving an approximate analytical solution to Eq. (15). This might be useful and is then the subject of the current investigation.

As most of the mathematical analyses reported so far on this problem, the present contribution assumed a lossless link. Besides being a common natural first step, this can also be justified by pointing out, as briefly done above, that in agreement with Smith *et al.* [21], we observed numerically that many of the properties found for a lossless link can be recovered in the presence of loss by an appropriate increase in the launch power of the transmitter. This is, however, system dependent (see, for example, Ref. [22], and references therein) and a separate analysis would be required for a clear picture.

ACKNOWLEDGMENTS

This research was supported by the Natural Science and Engineering Research Council (NSERC) of the Government of Canada and by the Fonds pour la formation de chercheurs et l'aide à la recherche (FCAR) du Gouvernement du Québec.

[1] N. J. Smith, N. J. Doran, W. Forysiak, and F. M. Knox, J. Lightwave Technol. **15**, 1808 (1997), and references therein.

[2] A. Hasegawa, Y. Kodama, and A. Maruta, Opt. Fiber Technol.: Mater., Devices Syst. **3**, 197 (1997), and references therein.

[3] M. Suzuki, I. Morita, N. Edgawa, S. Yamamoto, H. Taga, and S. Akiba, Electron. Lett. **31**, 2027 (1995); S. Kumar and F. Lederer, Opt. Lett. **22**, 1870 (1997); J. N. Kutz and P. K. A. Wai, IEEE Photonics Technol. Lett. **10**, 702 (1998); R.-M. Mu, V. S. Grigoryan, C. R. Menyuk, E. A. Golovchenko, and A. N. Pilipetskii, Opt. Lett. **23**, 930 (1998).

[4] M. Suzuki, I. Morita, N. Edagawa, S. Yamamoto, and S. Akiba, Electron. Lett. **33**, 691 (1997); E. Kolltveit, J.-P. Hamaide, and O. Audoin, *ibid.* **32**, 1858 (1996); W. Forysiak, J. F. L. Devaney, N. J. Smith, and N. J. Doran, Opt. Lett. **22**, 600 (1997); E. A. Golovchenko, A. N. Pilipetskii, and C. R. Menyuk, *ibid.* **22**, 1156 (1997); T.-S. Yang, W. L. Kath, and S. K. Turitsyn, *ibid.* **23**, 597 (1998); T. Hirooka and A. Hasegawa, *ibid.* **23**, 768 (1998); A. M. Niculae, W. Forysiak, A. J. Gloag, J. H. B. Nijhof, and N. J. Doran, *ibid.* **23**, 1354 (1998); D. J. Kaup, B. A. Malomed, and J. Yang, *ibid.* **23**, 1600 (1998).

[5] V. S. Grigoryan and C. R. Menyuk, Opt. Lett. **23**, 609 (1998).

[6] J. N. Kutz and S. G. Evangelides, Opt. Lett. **23**, 685 (1998).

[7] S. K. Turitsyn and E. G. Shapiro, Opt. Lett. **23**, 682 (1998).

[8] A. Bernston, N. J. Doran, W. Forysiak, and J. H. B. Nijhof, Opt. Lett. **23**, 900 (1998).

[9] Y. Chen and H. A. Haus, Opt. Lett. **23**, 1013 (1998).

[10] J. H. B. Nijhof, W. Forysiak, and N. J. Doran, Opt. Lett. **23**, 1674 (1998).

[11] T. I. Lakoba, J. Yang, D. J. Kaup, and B. A. Malomed, Opt. Commun. **149**, 366 (1998).

[12] S. K. Turitsyn, N. F. Smyth, and E. G. Turitsyna, Phys. Rev. E **58**, R44 (1998).

[13] J. H. B. Nijhof, N. J. Doran, W. Forysiak, and A. Bernston, Electron. Lett. **34**, 481 (1998).

[14] P. Fendley, A. Ludwig, and H. Saleur, Phys. Rev. B **52**, 8934 (1995).

[15] I. Affleck and A. Ludwig, J. Phys. A **21**, 5375 (1994).

[16] C. Paré and P.-A. Bélanger, in *Nonlinear Guidead Waves & Their Applications*, Vol. 5 of 1998 OSA Technical Digest Series (Optical Society of America, Washington, D.C., 1998), pp. 39–41.

[17] Here, the status of the integrability of the system is somewhat unusual. The original system is equivalent to a NLS equation with a periodic z-dependent dispersion and this is *not* integrable. On the other hand, the coupled system defined on $0<z<l$ by itself appears to be integrable; conservation laws are easily written down as linear combinations of two independent NLS conservation laws. However, when viewed in terms of the original variables, these are not local but rather *bilocal* as $\psi_{\pm}$ depends formally on z and $l-z$. Clearly, the integrability aspect requires further clarification.

[18] M. J. Ablowitz and G. Biondini, Opt. Lett. **23**, 1668 (1998).

[19] The multiple-scale method has also been used to analyze a dispersion-managed system, in a different regime, in T.-S. Yang and W. L. Kath, Opt. Lett. **22**, 985 (1997).

[20] A. Berntson, D. Anderson, N. J. Doran, W. Forysiak, and J. H. B. Nijhof, Electron. Lett. **34**, 2054 (1998).

[21] N. J. Smith, N. J. Doran, F. M. Knox, and W. Forysiak, Opt. Lett. **21**, 1981 (1996).

[22] T. Yu, R.-M. Mu, V. S. Grigoryan, and C. R. Menyuk, IEEE Photonics Technol. Lett. **11**, 75 (1999).